Robust optimization of ORC turbine cascades operating with siloxane MDM

Nassim Razaaly, Giulio Gori, Olivier Le Maitre, Gianluca Iaccarino, Pietro Marco Congedo

Robust optimization of ORC turbine cascades operating with siloxane MDM

By N. Razaaly†, G. Gori†, O. Le Maître¶, G. Iaccarino AND P.M. Congedo†

This work presents the application of a robust optimization approach to improve the efficiency of an Organic Rankine Cycle (ORC) cascade subject to uncertain operating conditions. The optimization algorithm is based on the minimization of a high quantile of a random cost function. The system under consideration employs siloxane MDM (Octamethyltrisiloxane) as a working fluid. The thermodynamic behavior of MDM requires the utilization of complex Equations-of-State (EoS) that rely on material-dependent parameters. Discussed here are the aleatory uncertainties affecting both the cascade operating conditions and the fluid model parameters. An uncertainty quantification framework is used to forward propagate the considered uncertainties to some performance estimators. The performances of the robust blade design are compared against performances characterizing the optimal design obtained using a deterministic optimization approach. Results show that the quantile-based approach yields to a significant improvement in cascade performance in variable operating conditions.

1. Introduction

Organic Rankine Cycle (ORC) applications take advantage of low-quality heat sources such as solar energy ponds, waste heat recovery, biomass combustion, etc, to convert the recovered heat into useful work. ORCs operate at high-pressure conditions, in the order of the critical point, and close to the liquid-vapor equilibrium curve. Under such conditions, organic compounds do not abide by the well-known Ideal Gas law. Namely, the thermodynamics admits different complex phenomena that are of the utmost relevance for industrial applications. For instance, the non-ideal decrease of the flow Mach number in supersonic expansions (Cramer & Best 1991), the non-ideal evolution of the Mach number in diabatic supersonic nozzle flows (Schnerr & Leidner 1991) and the Mach number increase across non-ideal oblique shock waves (Gori *et al.* 2017*a*; Vimercati *et al.* 2018). Besides ORCs, non-ideal effects are also relevant to supercritical CO_2 power systems, refrigerating systems, chemical or pharmaceutical industry and to many other applications (Colonna *et al.* 2008*b*; Congedo *et al.* 2011*a*; Wheeler & Ong 2013; Colonna *et al.* 2015).

Non-ideal flows are a novel research topic and may questions still remain to be addressed. For instance, the design of ORC devices relies largely on numerical tools and techniques developed for ideal fluids only. Moreover, the few available experimental data are affected by large uncertainties (Cinnella *et al.* 2010, 2011; Merle & Cinnella 2015),

† DeFI Team (INRIA Saclay Île-de-France, Ecole Polytechnique), Centre de Mathématiques Appliquées (CMAP), France

† DeFI Team (INRIA Saclay Île-de-France, Ecole Polytechnique), Centre de Mathématiques Appliquées (CMAP), France

¶ LIMSI, CNRS, Université Paris-Saclay, France

† DeFI Team (INRIA Saclay Île-de-France, Ecole Polytechnique), Centre de Mathématiques Appliquées (CMAP), France

making the development of high-fidelity EoS highly questionable (see Congedo *et al.* (2011*a*)).

Fluid-dynamic Shape Optimization (FSO) approaches offer the possibility of dealing with complex optimization problems at a reduced computational cost (Pironneau 1974). Those methodologies are perfectly suited to ORC applications, for which there is little design experience and limited experimental information (Harinck *et al.* 2013). Gradient-based and gradient-free algorithms were successfully applied to carry out the deterministic optimization of ORC nozzles and turbine blades (see Pini *et al.* (2015, 2014); Vitale *et al.* (2017); Rubino *et al.* (2018)).

Nevertheless, in ORC applications, the low quality of the heat and cold sources often result in significant variations of the fluid conditions at the turbine inflow and outflow. Clearly, the robustness to operating conditions variability must be taken into account at an early stage in the development process. In this context, Lee & Park (2006) propose a Robust Optimization (RO) formulation based on the minimization of a target performance variance. In Janusevskis & Le Riche (2013), the mean performance optimization is achieved through a Bayesian Optimization (BO) framework exploiting a Gaussian-Process (GP) -based model. Moreover, multi-objective optimization (Congedo *et al.* 2013; Bufi *et al.* 2017; Bufi & Cinnella 2017) and a multi-point approach (Pini 2013) have been proposed for ORC optimization problems.

In this work, we present the application of a quantile-based Bayesian optimization framework in the context of ORC turbine blade optimization. This robust shape optimization approach is applied to a typical 2D ORC turbine cascade (Colonna *et al.* 2008*a*). Section 2 describes the turbine cascade and the parametrization adopted to control the geometry of the blade in the optimization process. In Section 3, we summarize and discuss the aleatory uncertainties affecting our model. Section 4 briefly presents the deterministic and the quantile-based formulations for the optimization problem. Finally, Section 5 reports and compares performances of blade designs obtained using the two different formulations.

2. Turbine blade model

The Biere is a famous ORC blade geometry which is typically employed in supersonic axial turbine stators. The Biere represents a reference two-dimensional benchmark case to test the design of devices operating with siloxane fluid MDM (Octamethyltrisiloxane, $C_8H_{24}O_2Si_3$). The blade profile is meant to obtain a convergent-divergent cascade passage which serves to accelerate the fluid up to a supersonic speed. Across the cascade, the fluid is expanded from superheated conditions close to the saturation line ($\mathrm{P}_{in}^{\mathrm{T}} = 8$ bar, $\mathrm{T}_{in}^{\mathrm{T}} = 545.15$ K) to a static pressure in the order of $P \approx 1$ bar. As the flow past the cascade is supersonic ($\mathrm{M} \approx 2$ at the blade trailing edge), compressibility effects play a key role. Indeed, because of the high Mach number achieved at the nozzle exit, a typical fish-tail shock pattern is generated downstream the trailing edge (see Saracoglu *et al.* (2013)). The presence of strong shocks past stator vanes may result in large losses and thus the design of the trailing edge region is critical to turbine efficiency (Denton & Xu 1989; Mee *et al.* 1990). Moreover, shock-waves propagate through the vane and usually interact with the boundary layer developing over the suction side of the neighboring blade, thus further compromising the efficiency of the cascade.

The numerical domain is periodic over the vertical axis (y) with a stagger spacing of 45 mm. The flow is simulated up to a distance of $0.5 - 0.6$ and 2 chord-lengths ahead

and past the blade, respectively. The Biere pressure and suction sides are parametrized using a unique B-spline curve of degree 3 (see Hoschek *et al.* (1993); Farin (2002)). In this work, the B-splines were defined over a total number of 30 Control Points (CP). Only a subset of 11 CPs, mostly located on the suction side and trailing edge, is moved to seek for the optimal blade shape. The motion of the selected CPs is allowed in the direction normal to the baseline geometry. The maximum displacement of each CP was limited to a predefined range of values. In the following, $\mathbf{x} \in \mathbb{R}^{11}$ will denote the vector collecting the displacement of each CP i.e., the design control variables.

3. Uncertainty treatment

Generally, ORC cascades are subject to a wide variability of the operating conditions. According to Pini (2013), the operating conditions, namely the total pressure ($\mathrm{P}^{\mathrm{t}}_{in}$) and total temperature ($\mathrm{T}^{\mathrm{t}}_{in}$) at the turbine inflow and the static pressure past the cascade ($\mathrm{P}^{\mathrm{s}}_{out}$), can be modeled as uniformly distributed variables. The random vector $\boldsymbol{\xi}$ is defined as $\boldsymbol{\xi} = [P^{\mathrm{t}}_{in}, T^{\mathrm{t}}_{in}, P^{\mathrm{s}}_{out}]^T$. Namely, $\mathrm{P}^{\mathrm{t}}_{in} \sim \mathcal{U}[7.6, 8.4]$ bar, $\mathrm{T}^{\mathrm{t}}_{in} \sim \mathcal{U}[541.15, 549.15]$ K and $\mathrm{P}^{\mathrm{s}}_{out} \sim \mathcal{U}[1, 2]$ bar. The nominal operating conditions is defined as $\boldsymbol{\xi}_0 = [8.0, 545.15, 1.072]^T$.

As mentioned, ORC systems take advantage of complex compounds that do not generally abide by the ideal gas law and thus more complex EoS are needed. Among others, hereinafter we will consider the Peng-Robinson (PR) thermodynamic model (Peng & Robinson 1976), which includes a set of material-dependent parameters: the fluid pressure and the temperature at the critical point (P_{cr} and T_{cr}, respectively) and the acentric factor ω. Several authors have provided discrepant reference values for the material-dependent parameters, and these translate into aleatory uncertainties on the PR fluid model. Moreover, under the polytropic gas assumption (i.e., the heat capacity is assumed to be constant with temperature), the PR EoS ultimately depends also on a fourth parameter, the specific heat ratio γ.

In this work, a first attempt to infer the true value of the PR fluid model parameters for MDM was carried out based on experimental data. However, the available measurements are still not sufficient (both in terms of quantity and quality) and little, if nothing, can be learned from them. Nevertheless, the performances of the Biere blade, at the conditions of interest here, are almost insensitive to the variability of the fluid parameters. Indeed, a thorough investigation carried out using the Reynolds-Averaged Navier-Stoke (RANS) model pointed out that the quantities of interest do not change significantly, even if the PR parameters are allowed to vary considerably (even pushing the limit of physical admissibility). This result has also been confirmed in the past (see Congedo *et al.* (2011*b*, 2013); Geraci *et al.* (2016)). Therefore, any uncertainty underlying the PR fluid model in not considered and the nominal parameters values, according to Thol *et al.* (2017), are used throughout the rest of this work.

4. Optimization framework

In this section we describe the optimization framework. First, we recall the standard formulation for deterministic and unconstrained design problems. We then introduce the quantile-based formulation used to design the optimal and robust Biere blade. Finally, we present the Uncertainty Quantification (UQ) framework needed to propagate the uncertainties on the operating conditions to the performance parameters, to assess the characteristics of the final blade design.

4.1. *Deterministic optimization*

The classical formulation for constrained optimization problems in a deterministic framework reads

$$\min_{\mathbf{x}\in\Omega} f(\mathbf{x}) \quad \text{s.t. } \mathbf{g}(\mathbf{x}) \leq 0. \tag{4.1}$$

The cost function f depends on the design vector $\mathbf{x} \in \Omega \subset \mathbb{R}^{11}$, corresponding to the vector of variables in the B-spline parametrization of the blade profile (see Section 2). The optimum must satisfy a set of n_c constraints $\mathbf{g} \in \mathbb{R}^{n_c}$. In this work, we consider only the unconstrained optimization problem, that is $n_c = 0$.

To solve the optimization problem, we rely on a classical Bayesian framework for Surrogate-Based Optimization (SBO), the popular Efficient Global Optimization (EGO) (Brochu *et al.* 2010). Specifically, we consider a sequential approach where GP-based surrogate models are built to approximate the objective function f. At each step of the sequence, a new design $\mathbf{x}$ is obtained maximizing the so-called Expected Improvement (EI), which expression analytically depends on the current GP surrogate. This approach permits both to identify promising regions of Ω (exploitation) and to explore portions of the design space characterized by high uncertainty on the GP surrogate. The Improvement is defined as

$$I(\mathbf{x}) = \max(0, f_{\min} - \hat{f}(\mathbf{x})), \tag{4.2}$$

where $f_{\min}$ is the current optimum of the objective function obtained while exploring the design space Ω and $\hat{f}(\mathbf{x})$ denotes the current Gaussian predictor of $f(\mathbf{x})$. Note that $I(\mathbf{x}) \in \mathbb{R}^+$ is random, since $\hat{f}(\mathbf{x})$ is an univariate Gaussian variable. Therefore, the new design point $\mathbf{x}^\star$ is found solving

$$\mathbf{x}^\star = \arg\max_{\mathbf{x}\in\Omega} EI(\mathbf{x}), \tag{4.3}$$

where $EI(\mathbf{x}) = \mathbb{E}_{\hat{f}(\mathbf{x})}[I(\mathbf{x})]$ is the so-called Expected Improvement and $\mathbb{E}_{\hat{f}(\mathbf{x})}$ the expectation operator related to the randomness of the gaussian predictor $\hat{f}(\mathbf{x})$. The analytical expression of the expected improvement in the case of Gaussian surrogates is given in Brochu *et al.* (2010).

Since the optimization problem in Eq. (4.3) involves the surrogate model $\hat{f}$ only, it can be solved by means of any advanced optimization procedure, e.g. using Covariance Matrix Adaptation (CMA) (Nikolaus Hansen 2018). A full CFD simulation is then performed at the new design point $\mathbf{x}^*$, providing the objective function value $f(\mathbf{x}^\star)$, and the surrogate model is subsequently updated. This procedure is repeated until either a stopping criterion on the optimum is met or the budget of CFD simulations is exhausted.

4.2. *Robust optimization: quantile minimization*

When we are dealing with a system affected by uncertainties, the objective function h also depends on random quantities, modeled as the random vector $\boldsymbol{\xi}$. A mono-objective formulation of the minimization under uncertainties would consist in replacing the random objective function by a statistics of $h(\mathbf{x}, \boldsymbol{\xi})$. One natural choice is to minimize the mean of the random function. The sole minimization of an expected cost function usually results in a non-robust optimum as it does not incorporate any variability in the cost due to the uncertain parameters. This observation suggests consideration of the minimization of composite objective functions combining the first two (or more) statistical moments of h. For instance, a robust optimization approach could aim at minimizing the mean of h while penalizing its variance with some weight. Finding appropriate weights is, however,

difficult and somewhat arbitrary and the performance and robustness of the resulting optimal design can be highly sensitive to the penalization selected, as pointed out in Cook & Jarrett (2017). In addition, the accurate estimation of high-order statistical moments often incurs high computational costs.

Therefore, here we follow a quantile-based robust optimization, which aims at minimizing a usually high quantile of $h(\cdot, \boldsymbol{\xi})$. The problem is formulated as follows

$$\min_{\mathbf{x}\in\Omega} q_\alpha[h(\mathbf{x}, \boldsymbol{\xi})], \tag{4.4}$$

where, for $\alpha \in (0, 1)$, we have denoted $q_\alpha[h(\cdot, \boldsymbol{\xi})]$ the α-quantile of $h(\cdot, \boldsymbol{\xi})$ defined as

$$\mathbb{P}_{\boldsymbol{\xi}}(h(\cdot, \boldsymbol{\xi}) < q_\alpha[h(\cdot, \boldsymbol{\xi})]) = \alpha. \tag{4.5}$$

This quantile-based minimization problem is solved using a nested approach, where for each proposed design point $\mathbf{x}$, the α-quantile is estimated using an adaptive sampling method. Briefly, for a fixed $\mathbf{x}$, we start building a GP surrogate in the stochastic space of $h(\mathbf{x}, \boldsymbol{\xi})$, based on an initial Latin Hypercube Sampling (LHS) sample set of N_{LHS} points. This sample set is then adaptively enriched with new points selected using a criterion designed to improve the surrogate accuracy for the evaluation of the targeted quantile value (see Schöbi *et al.* (2017)). Denoting $h_\alpha(\mathbf{x})$ the surrogate-based estimate of the α-quantile of $h(\mathbf{x}, \boldsymbol{\xi})$, the SBO method described above is used to solve Eq. (4.4), substituting the objective function f by h_α.

5. Results

In this section we present results for the optimization problem for the trailing edge shock reduction in a turbine stator cascade. The optimization is carried out considering an inviscid and adiabatic flow model governed by Euler's equations. The SU2 open-source suite (Economon *et al.* 2016) was used for the CFD simulations. We used a generalized Approximate Riemann solver (ARS), of Roe type, with the SU2's library of thermodynamic models for complex fluid flows in the non-ideal regime (Vitale *et al.* 2015; Gori *et al.* 2017*b*). An implicit Monotone Upstream-centered Schemes for Conservation Laws (MUSCL) scheme, with van Albada slope limiter, is used to ensure second-order accuracy and prevent spurious oscillations in the steady-state solution. Non-Reflecting Boundary Conditions (NRBC) (Giles 1990) are also implemented to suppress the non-physical reflection of acoustic pressure perturbations at inflow and outflow boundaries. Detailed convergence analyses (not shown) have been performed, leading to computational mesh of the flow domain with $36,000$ triangular elements, which represents a trade-off between accuracy and computational cost.

Following Rodriguez-Fernandez & Persico (2015), the optimization aims at minimizing the pressure deviations in an azimuthal section located at half an axial chord downstream the trailing edge. The pressure deviations are measured by ΔP, the spatial Root Mean Square (RMS) of the pressure within the considered section. We contrast two optimal designs: the deterministic design corresponding to the minimization of ΔP for the deterministic conditions, that is considering the objective function $f(\mathbf{x}) = \Delta P(\mathbf{x}, \boldsymbol{\xi}_0)$, and the 95% quantile-based robust optimization using $f(\mathbf{x}) = q_{0.95}[\Delta P(\mathbf{x}, \boldsymbol{\xi})]$.

In order to assess the validity of the study, an Uncertainty Quantification (UQ) is performed considering a LHS set of 100 samples in the stochastic space for the two optimized profiles, based on Euler and RANS simulations, the latters using the Menter's Shear Stress Transport (SST) model (see Menter, F.R. (1993)). For these viscous sim-

Design	Euler						RANS					
	ΔP [kPa]			Y [%]			ΔP [kPa]			Y [%]		
	μ	σ	q_{95}	μ	σ	q_{95}	μ	σ	q_{95}	μ	σ	q_{95}
Deterministic	16.2	10.1	29.9	13.8	7.2	26.5	16.0	9.7	28.6	17.8	6.8	29.7
Quantile-based	8.9	2.4	12.7	11.3	2.4	16.2	8.8	2.4	12.5	15.2	2.3	19.8

Table 1: Blade designs assessment. The table reports the averages, standard deviations and 95% quantiles of the pressure deviation (ΔP) and total pressure loss (Y) in uncertain conditions for the optimal designs obtained with the deterministic and robust optimization. Also shown are the results for the viscous flow model (RANS).

ulations, a refined hybrid mesh with approximately $180,000$ elements was employed to ensure sufficient resolution of the boundary layers. A Monte-Carlo Sampling (MCS) combined to a GP-surrogate permits to evaluate meaningful statistics of the Quantities of Interest (QoI) ΔP and the total pressure loss $Y = (P^{\mathrm{t}}_{in} - P^{\mathrm{t}}_{out})/(P^{\mathrm{t}}_{in} - P^{\mathrm{s}}_{out})$, reported in Table 1. The interest of the robust optimization is evidenced by confronting the statistics of ΔP for the deterministic and robust designs. Note that the robust design not only exhibits a lower quantile (12.6 against 29.9), as expected, but also a lower variance and mean value of the pressure RMS ΔP than for the optimal design for the nominal conditions, denoting the lack of robustness of the latter. As reported in the right part of Table 1, although optimized on the non-viscous flow model, the quantile-based design significantly improves the statistics of both ΔP and Y when evaluated using the physically more complex model.

To gain further understanding of the impact of the robust optimization, we present in Figure 1(a,b) the Probability Density Functions (PDF) of ΔP for the baseline geometry (prior to any optimization), the deterministic optimal design, the q_{95} robust design and for both the inviscid (a) Euler and viscous (b) RANS simulations. The deterministic and the quantile-based optimal designs have distributions of ΔP that are significantly displaced toward the lowest values (to the left), with lower mean values, compared to the nonoptimized baseline design. Comparing the distributions of the deterministic and quantile-based optima, the effect of the robustness is obvious: whereas the deterministic design has a rather flat distribution, the robust design not only has a lower mean and variance (as shown in Table 1) but also its support is much tighter.

Finally, Figure 2(a) reports the baseline (black curve), deterministic (red) and quantile-based (green) optimal blade profiles. We also report the corresponding local coefficients of variation (ratio of standard deviation to the mean value) of the Mach number M in the flow domain in Figure 2(b,c,d). Again, the reduction of the Mach number CoV for the robust design is significant compared to other designs, in particular in the wake of the blades past the cascade.

6. Conclusions

This work presents the application of a robust optimization procedure to the design of a typical ORC turbine cascade operating under uncertain conditions. The optimization method minimizes a high quantile of the random cost function. The quantile-based optimal design is compared to the design obtained from a deterministic optimization

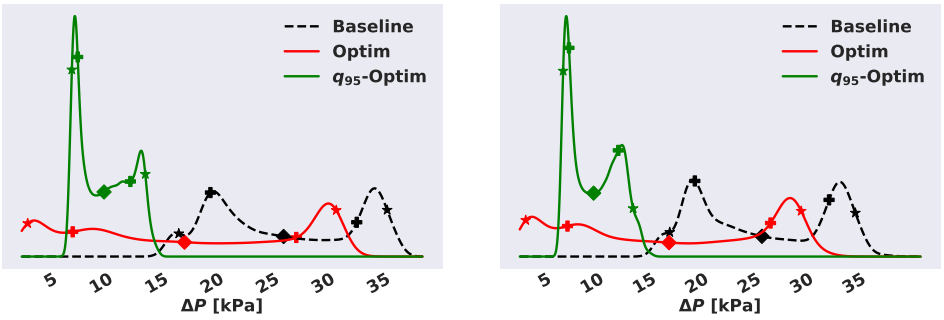

(a) (b)

Figure 1: PDFs of ΔP for the baseline (dashed curve), deterministic (red curve) and to the robust (green curve) designs. Diamonds mark the mean values μ, cross symbols indicate the $\mu \pm \sigma$ points, and stars mark the 5% and the 95% quantiles. The optimal designs are computed with Euler model, whereas the PDFs are estimated from (a) Euler and (b) RANS simulations.

for the nominal conditions. Results indicate that significant improvements are obtained using the quantile-based framework, with an optimal performance distribution having much lower mean and much compact support. Other quantities of interest, such as the Mach number and total pressure drop, benefit of the robustness although they were not directly optimized.

Acknowledgments

The authors acknowledge use of computational resources from the Certainty cluster awarded by the National Science Fundation to CTR. G. Gori and P.M. Congedo would like to thank the European Commission's H2020 programme, through the UTOPIAE Marie Curie Innovative Training Network, H2020-MSCA-ITN-2016, Grant Agreement number 722734.

REFERENCES

Brochu, E., Cora, V. & de Freitas, N. 2010 A tutorial on Bayesian optimization of expensive cost functions, with application to active user modeling and hierarchical reinforcement learning. *arXiv:1012.2599* .

Bufi, E. A., Camporeale, S. M. & Cinnella, P. 2017 Robust optimization of an organic Rankine cycle for heavy duty engine waste heat recovery. *Energy Procedia* **129**, 66 – 73, 4th International Seminar on ORC Power Systems, 2017, Milano, Italy.

Bufi, E. A. & Cinnella, P. 2017 Robust optimization of supersonic ORC nozzle guide vanes. *J. Phys. Conf. Ser.* **821** (1), 012014.

Cinnella, P., Congedo, P. & Parussini, L. 2010 Quantification of thermodynamic uncertainties in real gas flows. *Int. J. Engine. Systems Modelling and Simulation* **2** (1-2), 12–24.

Cinnella, P., Congedo, P., Pediroda, V. & Parussini, L. 2011 Sensitivity analysis of dense gas flow simulations to thermodynamic uncertainties. *Phys. Fluids* (23).

Colonna, P., Casati, E., Trapp, C., Mathijssen, T., Larjola, J., Turunen-

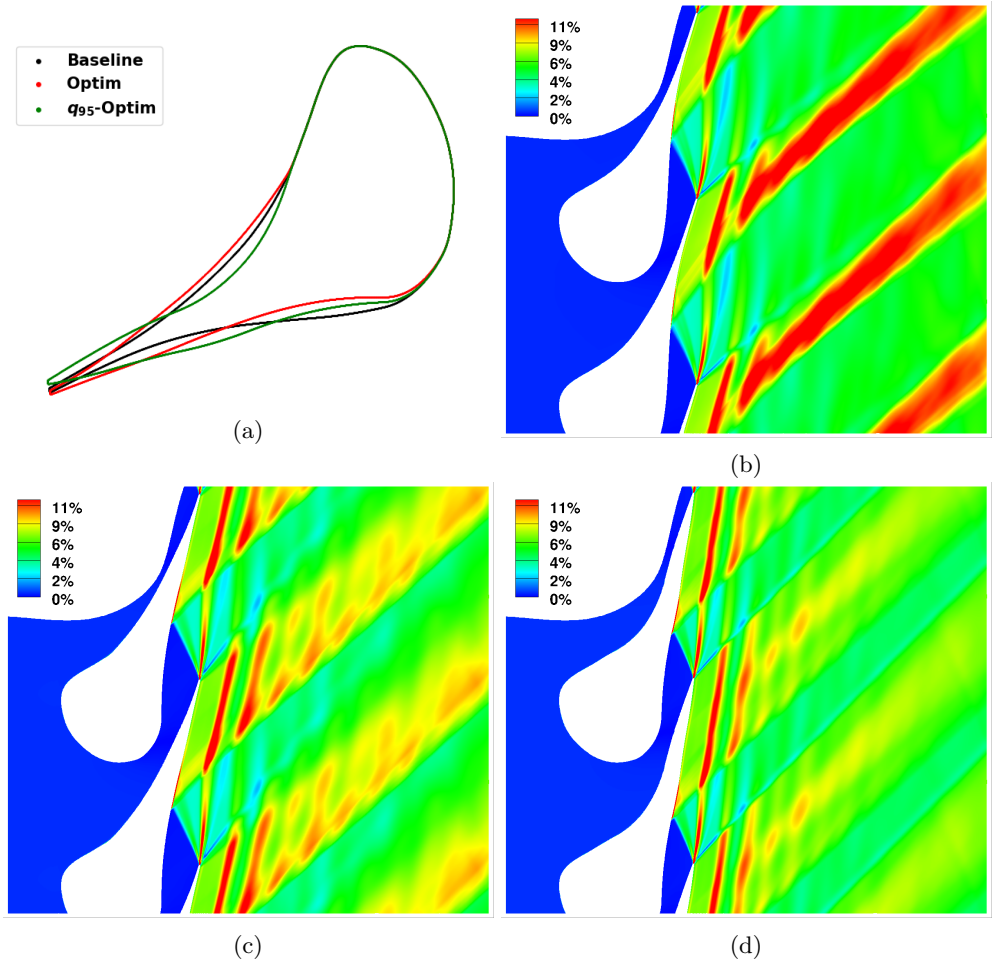

Figure 2: (a) Comparison of the baseline (black), deterministic (red) and robust (green) blade designs. Coefficients of Variations of the Mach number for the baseline (b), deterministic (c), and robust (d) designs. CoVs are computed with the RANS Model.

Saaresti, T. & Uusitalo, A. 2015 Organic Rankine Cycle power systems: From the concept to current technology, applications, and an outlook to the future. *J. Eng. Gas Turb. Power* **137** (10).

Colonna, P., Harinck, J., Rebay, S. & Guardone, A. 2008*a* Real-gas effects in organic Rankine cycle turbine nozzles. *J. Propul. Power* **24** (2), 282–294.

Colonna, P., Nannan, N. R. & Guardone, A. 2008*b* Multiparameter equations of state for siloxanes:$[(CH_3)_3 - Si - O_{1/2}]_2 - [O - Si - (CH_3)_2]_{i=1,...,3}$, and $[O - Si - (CH_3)_2]_6$. *Fluid. Phase Equilibr.* **263** (2), 115–130.

Congedo, P., Corre, C. & Cinnella, P. 2011*a* Numerical investigation of dense-gas effects in turbomachinery. *Comput. & Fluids* **49** (1), 290–301.

Congedo, P., Corre, C. & Martinez, J.-M. 2011*b* Shape optimization of an airfoil in a BZT flow with multiple-source uncertainties. *Comput. Method Appl. M.* **200** (1-4), 216–232.

Congedo, P., Geraci, G., Abgrall, R., Pediroda, V. & Parussini, L. 2013 TSI metamodels-based multi-objective robust optimization. *Eng. Computations (Swansea, Wales)* **30** (8), 1032–1053.

Cook, L. W. & Jarrett, J. P. 2017 Horsetail matching: a flexible approach to optimization under uncertainty. *Eng. Optimiz.* **50** (4), 549–567.

Cramer, M. S. & Best, L. M. 1991 Steady, isentropic flows of dense gases. *Phys. Fluids A* **3** (4), 219–226.

Denton, J. & Xu, L. 1989 The trailing edge loss of transonic turbine blades. In *ASME 1989 International Gas Turbine and Aeroengine Congress and Exposition*.

Economon, T. D., Mudigere, D., Bansal, G., Heinecke, A., Palacios, F., Park, J., Smelyanskiy, M., Alonso, J. J. & Dubey, P. 2016 Performance optimizations for scalable implicit RANS calculations with SU2. *Comput. Fluids* **129**, 146 – 158.

Farin, G. 2002 *Curves and Surfaces for CAGD: A Practical Guide*, 5th edn. San Francisco, CA, USA: Morgan Kaufmann Publishers Inc.

Geraci, G., Congedo, P., Abgrall, R. & Iaccarino, G. 2016 High-order statistics in global sensitivity analysis: Decomposition and model reduction. *Comput. Method Appl. M.* **301**, 80–115.

Giles, M. B. 1990 Nonreflecting boundary conditions for Euler equation calculations. *AIAA Paper #* **28** (12), 2050–2058.

Gori, G., Vimercati, D. & Guardone, A. 2017*a* Non-ideal compressible-fluid effects in oblique shock waves. *J. Phys. Conf. Ser.* **821** (1).

Gori, G., Zocca, M., Cammi, G., Spinelli, A. & Guardone, A. 2017*b* Experimental assessment of the open-source SU2 CFD suite for ORC applications. *Energy Procedia* **129** (Supplement C), 256–263.

Harinck, J., Pasquale, D., Pecnik, R., van Buijtenen, J. & Colonna, P. 2013 Performance improvement of a radial organic rankine cycle turbine by means of automated computational fluid dynamic design. *Proceedings of the Institution of Mechanical Engineers, Part A: Journal of Power and Energy* **227** (6), 637–645.

Hoschek, J., Lasser, D. & Schumaker, L. L. 1993 *Fundamentals of computer aided geometric design*. AK Peters, Ltd.

Janusevskis, J. & Le Riche, R. 2013 Simultaneous kriging-based estimation and optimization of mean response. *J. Global Optim.* **55** (2), 313–336.

Lee, K.H. & Park, G.J. 2006 A global robust optimization using kriging based approximation model. *JSME International Journal Series C Mechanical Systems, Machine Elements and Manufacturing* **49** (3), 779–788.

Mee, D., Baines, N., Oldfield, M. & Dickens, T. 1990 An examination of the contributions to loss on a transonic turbine blade in cascade. In *ASME 1990 International Gas Turbine and Aeroengine Congress and Exposition*.

Menter, F.R. Zonal Two Equation $k-\omega$, Turbulence Models for Aerodynamic Flows. *AIAA Paper*.

Merle, X. & Cinnella, P. 2015 Bayesian quantification of thermodynamic uncertainties in dense gas flows. *Reliab. Eng. Sys. Safe.* **134** (Supplement C), 305–323.

Nikolaus Hansen 2018 CMA. `https://pypi.python.org/pypi/cma`.

Peng, D. Y. & Robinson, D. B. 1976 A new two-constant equation of state. *Ind. Eng. Chem. Fundam.* **15**, 59–64.

Pini, M. 2013 Turbomachinery design optimization using adjoint method and accurate equations of state. PhD thesis, Politecnico di Milano.

Pini, M., Persico, G. & Dossena, V. 2014 Robust adjoint-based shape optimization of supersonic turbomachinery cascades. In *ASME Turbo Expo 2014: Turbine Technical Conference and Exposition*. American Society of Mechanical Engineers.

Pini, M., Persico, G., Pasquale, D. & Rebay, S. 2015 Adjoint method for shape optimization in real-gas flow applications. *ASME J. Eng. Gas Turb. Power* **137** (3).

Pironneau, O. 1974 On optimum design in fluid mechanics. *J. Fluid Mech.* **64** (1).

Rodriguez-Fernandez, P. & Persico, G. 2015 Automatic design of ORC turbine profiles using evolutionary algorithms. *3rd International Seminar on ORC Power Systems* (133).

Rubino, A., Pini, M., Colonna, P., Albring, T., Nimmagadda, S., Economon, T. & Alonso, J. 2018 Adjoint-based fluid dynamic design optimization in quasi-periodic unsteady flow problems using a harmonic balance method. *J. Comput. Phys.*

Saracoglu, B., Paniagua, G., Sanchez, J. & Rambaud, P. 2013 Effects of blunt trailing edge flow discharge in supersonic regime. *Comput. Fluids* **88**, 200–209.

Schnerr, G. H. & Leidner, P. 1991 Diabatic supersonic flows of dense gases. *Phys. Fluids A* **3** (10), 2445–2458.

Schöbi, R., Sudret, B. & Marelli, S. 2017 Rare event estimation using polynomial-chaos kriging. *ASCE-ASME Journal of Risk and Uncertainty in Engineering Systems, Part A: Civil Engineering* **3** (2).

Thol, M., Dubberke, F. H., Baumhgger, E., Vrabec, J. & Span, R. 2017 Speed of sound measurements and fundamental equations of state for octamethyltrisiloxane and decamethyltetrasiloxane. *J. Chem. Eng. Data* **62** (9), 2633–2648.

Vimercati, D., Gori, G. & Guardone, A. 2018 Non-ideal oblique shock waves. *J. Fluid Mech.* **847**, 266–285.

Vitale, S., Albring, T. A., Pini, M., Gauger, N. R., Colonna, P. *et al.* 2017 Fully turbulent discrete adjoint solver for non-ideal compressible flow applications. *J. of the Global Power and Propulsion Society* **1**.

Vitale, S., Gori, G., Pini, M., Guardone, A., Economon, T. D., Palacios, F., Alonso, J. J. & Colonna, P. 2015 Extension of the SU2 open source CFD code to the simulation of turbulent flows of fluids modelled with complex thermophysical laws. *AIAA Paper*.

Wheeler, A. & Ong, J. 2013 The role of dense gas dynamics on organic Rankine cycle turbine performance. *J. Eng. Gas Turbines Power* **135** (10), 102603.